



HAL
open science

Structural integrity and skeletal trace elements in intertidal coralline algae across the Northeast Atlantic reveal a distinct separation of the leading and the trailing edge populations

Regina Kolzenburg, Hugo Moreira, Craig Storey, Federica Ragazzola

► To cite this version:

Regina Kolzenburg, Hugo Moreira, Craig Storey, Federica Ragazzola. Structural integrity and skeletal trace elements in intertidal coralline algae across the Northeast Atlantic reveal a distinct separation of the leading and the trailing edge populations. *Marine Environmental Research*, 2023, 190, pp.106086. 10.1016/j.marenvres.2023.106086 . hal-04732065

HAL Id: hal-04732065

<https://hal.science/hal-04732065v1>

Submitted on 13 Oct 2024

HAL is a multi-disciplinary open access archive for the deposit and dissemination of scientific research documents, whether they are published or not. The documents may come from teaching and research institutions in France or abroad, or from public or private research centers.

L'archive ouverte pluridisciplinaire **HAL**, est destinée au dépôt et à la diffusion de documents scientifiques de niveau recherche, publiés ou non, émanant des établissements d'enseignement et de recherche français ou étrangers, des laboratoires publics ou privés.



Distributed under a Creative Commons Attribution 4.0 International License



Structural integrity and skeletal trace elements in intertidal coralline algae across the Northeast Atlantic reveal a distinct separation of the leading and the trailing edge populations

Regina Kolzenburg^{a,b,*}, Hugo Moreira^{c,d}, Craig Storey^d, Federica Ragazzola^e

^a ENEA Marine Environment Research Centre, Via Forte Santa Teresa, 19032, Pozzuolo di Leri, SP, Italy

^b Institute of Marine Sciences, University of Portsmouth, Portsmouth, UK

^c Géosciences Montpellier CNRS, Université de Montpellier, 34090, Montpellier, France

^d School of the Environment, Geography and Geosciences, University of Portsmouth, Portsmouth, UK

^e Genova Marine Centre, Stazione Zoologica Anton Dohrn, Piazza del Principe, 4, 16126 Genova GE, Italy

ABSTRACT

Intertidal macroalgae, such as coralline algae, represent an essential structural element and substrate in rocky coastal zones. They have a high degree of flexibility allowing their survival in environments with severe mechanical stress during tidal cycles. This study characterised the genicula and intergenicula of the calcifying red alga *Corallina officinalis* across its geographic distribution in the Northeast Atlantic. Poleward populations have constructed more sturdy cell walls compared to equatorward populations, potentially due to greater local adaptations to higher frequency and intensity of environmental factors like storms and wave action. Southern populations showed a lack of local adaptation culminating in survival rather than thriving within their current environment, hence, they are located at the margin of this species' favourable conditions. Results clarify significant differences between latitudes and indicate a north-to-south gradient in this species' skeletal elemental composition. Northern populations were dominated by cadmium, whereas chromium was the major trace element found in southern populations. In the future, these characteristics could lead to a permanent decline and a decrease in the ecosystem functions of *C. officinalis* in the southern locations in the Northeast Atlantic, which may be accelerated by predicted future climatic changes.

1. Introduction

Marine calcifying organisms such as coralline red algae (Corallinales, Rhodophyta) are indispensable components of global marine shallow-water ecosystems (Adey and Macintyre, 1973; Steneck, 1986). Functioning as important ecosystem engineers they play a vital role as essential structural elements in rocky coastal zones by providing rigid substrates (Dayton, 1972; Johansen, 2018; Kelaher et al., 2001; Marchini et al., 2019; Noël et al., 2009).

To sustain their abundance in intertidal ecosystems, it is suggested that coralline algae have a good ability to adapt to great and fast changes in environmental conditions, such as solar irradiance, water temperature, physical stress or carbonate chemistry (e.g. considerable pH variations) which fluctuate seasonally, monthly, diurnally and tidally (Hofmann et al., 2014; Martone et al., 2010; Williamson et al., 2014). Besides the shallow-water ecosystem they dominate, these factors can impact their physiology and morphology. However, it is recognized that species with a wide geographical range, such as coralline algae, are very plastic and able to adjust to various habitats through morphological and

functional responses (Kolzenburg et al., 2021; McCoy and Widdicombe, 2019; Ragazzola et al., 2013).

Within coralline algae, at many wave-exposed sites, erect (geniculate) corallines are the dominant competitor for space in the low intertidal zone. Erect coralline algae habitually form dense, convoluted and highly branched turfs which are expressed to be extreme in algal structural complexity (Coull and Wells, 1983; Davenport et al., 1999). One example is *Corallina officinalis*, which forms turf across extensive ranges on hard substratum in the intertidal ecosystems of the Northeast Atlantic. Studies have shown that predicted future environmental conditions caused by climate change may have an opposing effect on *C. officinalis* throughout their latitudinal gradient. It is predicted that, physiologically, leading edge populations in high latitudes show a more resilient response to experimental thermal and stress levels, coping best with changes in pH and temperature as predicted in modelled future scenarios (IPCC, 2023) as compared to central and trailing edge populations (Kolzenburg et al., 2021). This could have a severe knock-on effect on biodiversity in *C. officinalis* dominated habitat, because without *C. officinalis*, ~ 80% of other organisms may not persevere in

* Corresponding author. ENEA Marine Environment Research Centre, Via Forte Santa Teresa, 19032, Pozzuolo di Leri, SP, Italy.

E-mail address: regina.kolzenburg@gmail.com (R. Kolzenburg).

coastal rocky shore habitats, leaving shores considerably depleted in diversity (Grahame and Hanna, 1989). Ultimately, this should be taken into consideration when designing protected areas or policies around coastal species conservation due to the immense effect a continuous loss of this and closely related species may have on coastal productivity.

Turf beds produced by geniculate coralline algae can be highly variable in frond length and density which could be related to a shift in their energy budget from growth extension to preservation of structural integrity (Ragazzola et al., 2013). Due to the nature of its habitat in the rocky shore intertidal zones erect coralline algae are exposed to tremendous wave action and powerful seawater velocities ($>20 \text{ m s}^{-1}$) (Denny, 1988). They evolved c. 100 Ma by developing flexible thalli consisting of multiple calcified intergenicula arising from one another, connected by a non-calcified genicula, acting as joints (Fig. 1; Aguirre et al., 2010). This structure provides flexibility and elasticity for every individual thallus (Martone and Denny, 2008a). A system of thalli growing from one initial point on the holdfast disc forms a frond. The intergenicula size and shape are characteristic of certain genera or species but can be influenced by external factors such as abiotic or biotic stressors (Johansen, 2018). The cell geometry and cell wall and genicula composition can also influence the stress and strain of the structure of articulated coralline algae (Martone, 2007; Martone et al., 2019).

Several studies have investigated the mechanical properties of the genicula, which are four times stronger and six times as extensible as fleshy algae (Janot and Martone, 2016; Martone, 2007), and resistant to fatigue of a single thallus. These studies were ground-breaking in understanding how geniculate algae can grow to sizes that would not be possible considering the hydrodynamic forces they face, which are potentially able to break or dislodge them (Denny, 1988, 1995; Denny and Wethey, 2001). However, very few studies have attempted to compare the resistance (via tensile stress) of frond bundles (Ragazzola et al., 2017) and no study compared the mechanical properties of the same coralline species across different environments. This knowledge is crucial to determine how and whether the wider distributed, turf-forming algae *C. officinalis* will be able to withstand climatic

changes and with it, an increase in intensity and frequency of physical force exposure caused by coastal storm events.

The calcified intergenicula of coralline algae are made of high-magnesium (Mg) calcite deposited inside the cell wall. Mg is the most studied element in coralline algae, especially for temperature reconstruction (Milliman et al., 1971). Coralline algae, amongst others, can contain between 7.7 and 28.8 mol% Mg-calcite (Chave, 1954a, 1954b; Halfar et al., 2000; Kamenos et al., 2008; Vinogradov, 1953). A concentration of around 8 mol% would translate to approximately 2% of Mg in relation to the total weight, making coralline algae the main producer of high-Mg calcite in the ocean (Johansen, 2018). Mg concentrations in the thallus vary and are directly or indirectly influenced by growth rates, light, physiological cycles and mostly temperature (Chave and Wheeler Jr, 1965; Moberly Jr, 1968). The substitution of Mg into calcite is an endothermic reaction, hence, the Mg/Ca ratio of calcite is expected to increase with increasing temperature (Lea et al., 1999; Rosenthal et al., 1997), with a temperature dependence of Mg uptake into calcite of up to 3 mol% per 1°C . A high Mg content may also improve the mechanical properties of biogenic minerals (Long et al., 2014). Mg is not the only element which is incorporated into the organisms' calcite lattice (Table 1; Halfar et al., 2000; Saha et al., 2016) and previous studies have measured trace elements such as strontium (Sr) and barium (Ba) (Johansen, 2018; Milliman et al., 1971). These elements in coralline algae provide important information about changes in environmental and compositional parameters of the ambient seawater at the time of growth. Trace elements such as iron (Fe), sodium (Na), and manganese (Mn) have been used to determine and reconstruct historically physiological performance and environmental metal contamination (Darrenougue et al., 2018; Raven et al., 1999) while in fleshy algae, other elements are used for more generic physiological and environmental proxies and pollution assessment (cadmium (Cd), chromium (Cr), vanadium (V) and zinc (Zn); Tuzen et al., 2009; Table 1). Coralline algae used as an environmental reconstruction proxy are typically non-geniculate, long-lived organisms forming annual bands. Therefore, very little knowledge of trace elements in geniculated coralline algae is

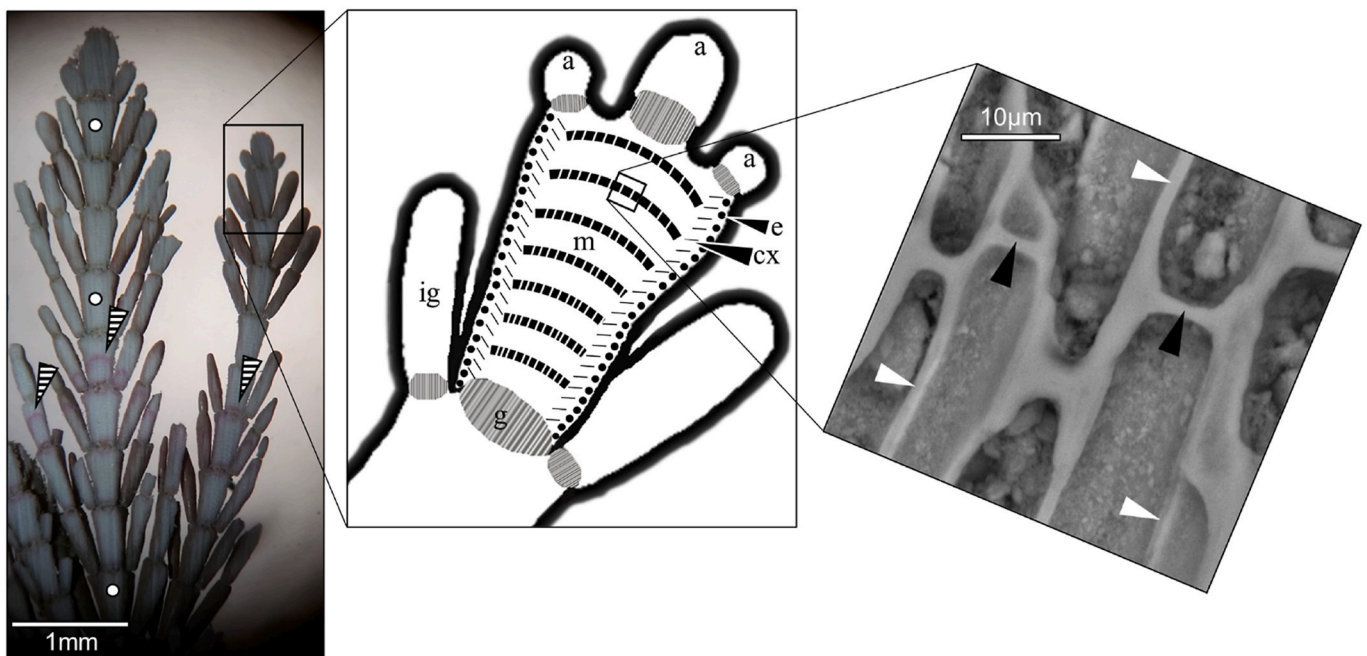


Fig. 1. Structure of *Corallina officinalis*. Left: full thalli with Alizarin Red S staining (striped arrows) and representative location of lower, middle and upper thallus region (white circles). Middle: schematic of structural elements and cell specification: calcified intergenicula segments (ig) alternating with non-calcified genicula segments (g), a meristematic apex (a); an intergeniculum consisting of a central medulla (m), a peripheral cortex (cx) and an epidermis (e) covered with a cuticle. Cell walls form a banding pattern with smaller, more calcified cells formed in winter and larger, less calcified cells formed in summer. Right: scanning electron microscopy image showing intra (parallel to growth direction) cell walls (white arrows) and inter (perpendicular to growth direction) cell walls (black arrows).

Table 1
Elements as proxies for biotic and abiotic environmental and physiological factors.

Element	Proxy	Correlation (concentration vs. effect)	Skeletal form of calcium carbonate	Organism	Reference	
Barium	Ba	Salinity & freshwater and sediment discharge	Calcite	Corallinaceae	(Chan et al., 2011; Johansen, 2018; Milliman et al., 1971)	
Cadmium	Cd	Pollution through anthropogenic input, reduced cell wall viability, DNA damage and inhibition of calcite precipitation and primary production	N/A Calcite N/A	Cyanophyceae, Chlorophyceae Corallinaceae Higher plants	Vymazal (1987) Kangwe et al. (2001) Nazar et al. (2012)	
Chromium	Cr	DNA and gene transcription modification, cancerogenic, growth and primary production inhibitor	N/A Primarily aragonite	Fleshy Rhodophyta Scleractinian corals	Sari and Tuzen (2008) Pereira et al. (2016)	
Iron	Fe	Electron transport in photosynthetic and respiratory processes	Calcite	Oxygen-evolving organisms (e. g. higher plants, algae, Cyanophyceae, diatoms, etc.) Corallinaceae	Raven et al. (1999) (Johansen, 2018; Milliman et al., 1971)	
Magnesium	Mg	Contamination		Sporolithales rhodoliths	Darrenougue et al. (2018)	
		Temperature	Direct, neutral Direct, positive	Primarily calcite Corallinaceae	(Halfar et al., 2000; Johansen, 2018; Milliman et al., 1971)	
Strontium	Sr	Salinity incl. Historical reconstruction	Direct, positive	Primarily aragonite Corallinaceae Aragonitic bivalve shells (<i>Arctica islandica</i>)	Johansen (2018) Schoene et al. (2010)	
Vanadium	V	Catalyst for amino acid production & chlorophyll <i>a</i> formation, enzyme activity	Direct, positive	N/A Chlorophyta (freshwater)	(Meisch and Bauer, 1978; Meisch and Benzschawel, 1978; Wilhelm and Wild, 1984a, 1984b)	
Zinc	Zn	Efficiency of photosynthetic reactions, CO ₂ assimilation, enzyme and protein build-up	Direct, positive	Calcite Calcite	Corallinaceae Oxygen-evolving organisms (e. g. higher plants, algae, cyanobacteria, diatoms, etc.)	Krenn et al. (1989) Raven et al. (1999)
				N/A	Fleshy Pheophyceae, Chlorophyta, Rhodophyta	Amado Filho et al. (1997)
		Growth inhibition & fatal toxicity at high concentrations	Direct, negative	N/A	Higher plants	Rout and Das (2009)

published, mostly because fronds are fragile, shorter-lived than crusts, and therefore may not allow for precise, long-ranged historic reconstruction. Nevertheless, they can still provide fundamental information on the environmental status of their habitat and, linked with physiological assessment, on organismal metabolic performance.

This study represents a characterization of the structural integrity and trace elemental composition of *C. officinalis* across its natural distribution in the NE Atlantic. Environmental status of the habitat aside, we hypothesise that central populations are structurally more robust to environmental conditions and, thus, may show less differences in measurements such as elemental ratios, growth rates, cell wall thickness, tensile strength, strain and stress. In contrast, we predict that northern and southern populations will present greater differences within their skeletal chemical composition and mechanical properties, indicating their resilience to predicted higher *in situ* fluctuations of physical forces and temperatures.

2. Material and methods

2.1. Species collection

Specimens of two *Corallina officinalis* populations per country were collected intertidally, during low tide at a depth of ~0.25m from the water surface at sites in South East England (central populations CP1 & CP2; January 2017 & July 2017), North West Spain (trailing edge populations SP1 & SP2; February 2017 & July 2018) and South West Iceland (leading edge populations NP1 & NP2; November 2017 & July 2017; Table 2) in summer and in winter. Specimens from all locations were genetically identified in previous studies (Kolzenburg et al., 2019; Tavares et al., 2018). Field sites and sampling times are identical to those described previously (Kolzenburg et al., 2023). Only healthy individuals without damage or bleaching were selected. Samples were

Table 2
Sampling site coordinates.

	Site name	Coordinates	Beeline distance between populations
Northern population 1	Stafnes South	N 63.968444,	1.59 km
		W 22.750861	
Northern population 2	Stafnes North	N 63.974380,	26.85 km
		W 22.753610	
Central population 1	St Margarets Bay	N 51.148056,	7.19 km
		E 1.385056	
Central population 2	Westbrook Bay	N 51.388840,	
		E 1.367170	
Southern population 1	Illa del Arousa	N 42.56870,	
Southern population 2	Tragove	W 8.89171	
		N 42.52444,	
		W 8.82772	

collected, cleaned from epibionts and some were kept in temperature-controlled chambers with regular water change, others were dried for 48 h at 60 °C before transportation to the laboratories of the University of Portsmouth for structural and elemental analysis.

2.2. Measurements of environmental parameters

Temperature, salinity, dissolved oxygen (DO), pH, irradiance and total alkalinity (A_T) were measured ($n = 1$ in 2016, $n = 3$ in 2017 and 2018) during sample collection (Table S1).

2.3. Tensile strength

Ultimate tensile strength (F_{tu}) is defined as the material's capacity to withstand loads elongating the specimen and subsequently determining the strength and resistance to tension. Investigated in this study is the genicula, the predominant breaking point during tensile strength.

Tensile strength was measured in a wet chamber filled with filtered seawater for only two populations, NP1 and CP1, for one season each (winter and summer, respectively).

Wet samples ($n = 20$ and 40 for NP1 and CP1, respectively) were fixed to a 2 cm, flat wooden surface, using instant adhesive. For consistency and comparability, only the top and the bottom three calcified intergenicula segments of all 1.00 ± 0.13 cm long specimens were attached. It was ensured the tested sample length was not contaminated with adhesive to prevent alterations of structural properties.

Wet samples were conducted using an ElectroForce fatigue test instrument (Model 3220 Series II, Bose Corporation, Eden Prairie, MN, USA) and analysed using the WinEst 7 software (Bose Corporation, Eden Prairie, MN, USA), analytic settings can be found in Table S2. Data were plotted and analysed using Excel (Microsoft Office, USA). Measurements for Load were plotted against displacement, indicating the tension needed to break each sample. In addition, Strain, representing the material extensibility of each sample, was added to the same figure. The strain was calculated using the following equation:

$$\epsilon = \frac{\Delta L}{L_0}$$

with ΔL as the change in sample length [mm] and L_0 as the initial sample length [mm].

Additionally, an estimation of stress (σ , $N\ mm^{-2}$) on the broken geniculum obtained from dry specimens ($n = 30$ and 20 for NP and CP, respectively) of the same location but from a different time point was calculated following the equation

$$\sigma = \frac{F_{tu}}{A_{geniculum\ cross-section}}$$

with $A_{geniculum\ cross-section}$ representing the area in mm^2 .

2.4. Cell wall thickness (CWT)

Using scanning electron microscopy (SEM) the cell wall structure of 3 specimens, $n = 15$ measurements for each per season and site, was measured (total count of 540 measurements). Analyses were focused on different heights of the centre of the medulla tissue within the thallus (Fig. 1) to ensure full calcification.

An Environmental SEM was used (EVO MA10 with a W filament electron source, Zeiss, Oberkochen, Germany) enabling the use of the same mounts for LA-ICP-MS and SEM analysis without the interference of sample coating. Sample mounts were fixed on stabs with double-coated carbon conductive tabs and cleaned using Isopropanol, before being placed into the SEM under a variable pressure (VP) vacuum of 28 Pa.

Images were taken at 20 kV electron high tension (EHT) accelerating voltage with a probe of 300 pA, a working distance (WD) of 7–9 mm, a scan speed of 20.5 s, a magnification of 3 K and a Backscatter line average noise reduction (HDBSD) mode. ImageJ (Rasband, 2016) was used to determine the intra- (parallel to growth direction) and inter-cell wall (perpendicular to growth direction) thickness (CWT) of specimens.

2.5. Linear growth rates

Growth rates were determined using transplants of *C. officinalis* at sampling sites of NP1 and CP1 (Table 2). A transplant of SP had been planted into the field but was not recoverable. Specimens were carefully removed using a hammer and chisel ensuring complete removal

including the encrusting base. They were submerged into a solution of $0.5\ g\ L^{-1}$ Alizarin Red S vital stain (Fluks, Sigma-Aldrich, Steinheim, Germany) for 24 h under a light intensity of $\sim 35\ \mu mol\ m^{-2}\ s^{-1}$ (Andrake and Johansen, 1980). After staining, algae were carefully and thoroughly rinsed with filtered seawater. The following day, specimens were placed back at the point of collection, using epoxy resin (Splash Zone A-788, KOP-COAT, Inc., NJ, USA) to attach the holdfast. Transplants were collected after 3 months in northern (late July – early November) and 5 months in central locations (late January – early July), specimens were carefully dried and growth rates were determined (Kolzenburg et al., 2021). Analyses consisted of 298 northern and 118 central replicates.

2.6. Trace element composition

Element/Ca ratios within the calcite were determined by laser ablation inductively coupled plasma mass spectrometry (LA-ICP-MS). Chosen elements included: Magnesium (Mg), Vanadium (V), Chromium (Cr), Zinc (Zn), Strontium (Sr), Cadmium (Cd) and Barium (Ba). Ablations were focused on the medulla tissue to ensure full calcification (Fig. 1).

Replicate thalli from different individuals ($n = 3$) of each population were embedded into epoxy resin (EpoFix Kit, batch no: 8134–01, Struers ApS, Ballerup, Denmark) and polished (MetaServ 3000 or Vibromet 2, Buehler, Esslingen, Germany) using an aluminium oxide solution of $0.05\ \mu m$ grain size (Micropolish Alumina, Buehler, Esslingen, Germany).

Analyses were conducted at the School of Earth and Environmental Sciences, University of Portsmouth, using a RESolution 193 nm ArF excimer Laser with a Laurin Technic S155 Ablation cell coupled to an Analytic Jena Plasma Quant MS Elite ICP-MS (Table S3). Analyses were performed using a $55\ \mu m$ spot size, laser fluency of $3.0\ J\ cm^{-2}$ and a repetition rate of 5 Hz. Background measurements of 20 s were followed by 30 s of ablation and 15 s of washout for each analysis. The following masses were measured with a 10 ms integration time: ^{26}Mg , ^{44}Ca , ^{43}Ca , ^{51}V , ^{52}Cr , ^{57}Fe , ^{66}Zn , ^{88}Sr , ^{111}Cd , ^{137}Ba .

Background and signal counts were integrated, time-drift corrected and reduced to concentrations using the software Iolite 3.4 (Paton et al., 2011). Synthetic silicate glass reference materials NIST SRM (National Institute of Standards and Technology Standard Reference Material) 610 and NIST SRM 612 were used for instrumental calibration and as primary and secondary standards. Synthetic calcium carbonate USGS (United States Geological Survey) MACS-3 was also used as a secondary standard and analysed using the same conditions as the samples. Each run consisted of at least six external standard analyses (NIST 610) and four secondary standards NIST 612 and MACS-3 ($n = 8$). Detection limits (99% confidence) for spot measurements of NIST glasses were: $Mg = \sim 28\ ppm$ and $Ca = \sim 100\ ppm$.

The internal standard element for normalization of the data was ^{43}Ca , obtained from the GeoReM (Geological and Environmental Reference Materials) database and own measurements. All reference materials were ablated before, in the middle of and after sample ablations. Following every sixth sample analysis, one analysis of NIST SRM 610 was added to correct for time-dependent drift of mass discrimination and instrument sensitivity. Final elemental composition ratios were calculated as a 'mean count rate' including standard error of 9 drift and background corrected single ablation spot analysis for each of the three replicates. Spots ($n = 3$) were ablated at the lower, middle and upper regions of the selected thallus (Fig. 1). This method is commonly used for LA-ICP-MS data reduction (Longerich et al., 1996). Obtained values are reproducible within 10% for Mg, of the GeoReM recommended values (Jochum et al., 2005) and were compared for accuracy with the GeoReM database (Figs. S1 and S2) and for internal (NIST 610) and external reproducibility (MACS-3 and NIST 612; Table S4).

2.7. Data and statistical analysis

Data of tensile strength, intra- and inter-cell wall thickness and monthly linear growth rates of NP1 and CP1 (all $n = 118$) were not normally distributed or homogenous, so they were analysed using SPSS v.28 (IBM Corp, 2021), using independent-sample Kruskal-Wallis H tests with pairwise comparison.

Elemental data was analysed using PRIMER 6.1 (Anderson et al., 2009), after data normalization by fourth root transformation due to extremely high variability of elemental concentrations; a permutational analysis of variance (PERMANOVA) with country, population and seasons as factors and populations nested into country and 9999 permutations was performed. Additional similarity of percentage (SIMPER) analyses were performed to determine the major influential elements for lower thallus regions of each group. Fe was excluded from SIMPER analyses due to skewness caused by very high measurement sensitivity but remained incorporated in all other analyses.

3. Results

3.1. Tensile strength

The predominant breaking point was the non-calcified genicula, which is what is referred to when discussing the data.

Wet specimens of central populations under summer conditions were able to withstand an ultimate tensile strength (F_{tu}) of 0.886 ± 0.083 N (mean \pm SE, Fig. 2) which is not significantly different from wet northern populations under winter conditions (1.181 ± 0.080 N, Fig. 2). Neither displacement nor strain showed a significant difference between the two populations.

Results reveal a greater stress imposed on genicula of CP (46.53 ± 7.75 N mm^{-2} , mean \pm SE) as compared to NP (20.50 ± 2.02 N mm^{-2} , mean \pm SE).

3.2. Cell wall structure

Inter-CWT (Fig. 3; Table S5(A)) was significantly higher in NP compared to CP (1.30-times and 1.33-times for summer and winter respectively) and SP (1.21-times and 1.49-times for summer and winter respectively) in both seasons (Kruskal-Wallis H test, $P = 0.000$ for all; Table S5(B)). SP were the only populations that showed a significant difference in inter-CWT between seasons (Kruskal-Wallis H test, $P = 0.000$). In NP and CP inter-CWT was marginally thicker in winter than in

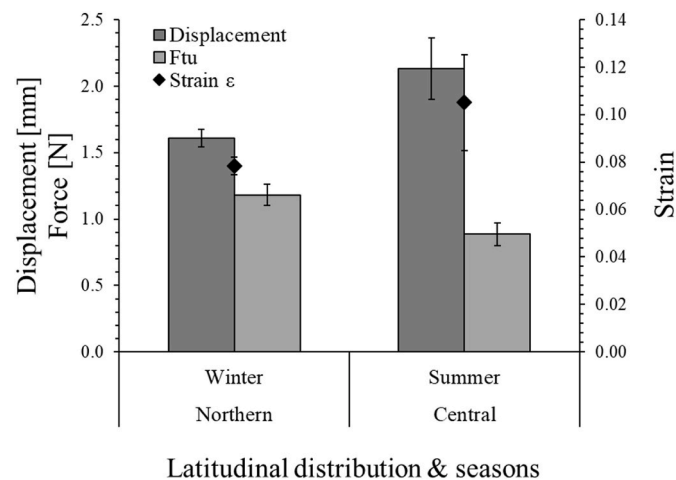


Fig. 2. Ultimate tensile strength (F_{tu}) [N], displacement [mm] and normal strain ϵ (mean \pm SE; $n = 20$ and 40 for northern and central populations, respectively) of wet *Corallina officinalis* across its distribution in the NE Atlantic in summer and winter.

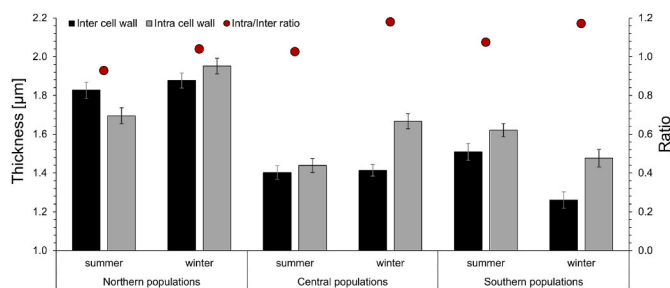


Fig. 3. Inter- and intra-cell wall thickness of *Corallina officinalis* samples in the field. Black and grey bars represent inter- and intra-cell wall measurements [μm], respectively. (mean \pm SE, $n = 15$). The left, middle and right sections of the graph represent the northern, central and southern regions, respectively. Within each region, populations ($n = 2$) are compared during summer and winter conditions.

summer. Intra-CWT was more variable than inter-CWT.

Like inter-CWT, intra-CWT showed a significant difference between NP (1.70 ± 0.04 μm and 1.95 ± 0.04 μm for summer and winter, respectively) and CP (1.44 ± 0.04 μm and 1.67 ± 0.04 μm for summer and winter, respectively) in both seasons (Kruskal-Wallis H test, $P = 0.000$ for all) while there was no significant difference between NP and SP in summer. All populations showed a significant difference in intra-CWT NP and CP increased from summer to winter whereas SP decreased from summer to winter.

3.3. Linear growth rates

Growth rates of NP were 2.08 ± 0.03 mm $month^{-1}$. Those of CP were significantly lower at 0.25 ± 0.03 mm $month^{-1}$ (Fig. 4; Kruskal-Wallis H test, $P < 0.001$). Staining success totals $\sim 57\%$ and $\sim 70\%$ for CP and NP, respectively.

3.4. Elemental composition of the skeleton

SIMPER analysis revealed a separation between NP and CP and NP and SP for Cd (Fig. 5) and a general trend towards dissimilarity between seasons of CP but not NP or SP.

Mg/Ca was only comparable between seasons in NP, but not in CP or SP where ratios significantly decreased with winter temperatures (Kruskal-Wallis H test, $P = <0.030$ for all thallus regions; Fig. 6, Tables S6 and S7). In all populations, independently of season, Mg/Ca ratios increased with tissue age, meaning from the upper towards the bottom thallus region. Comparing the thallus middle in summer by latitude, Mg/Ca ratios showed a significant increase from NP to CP and

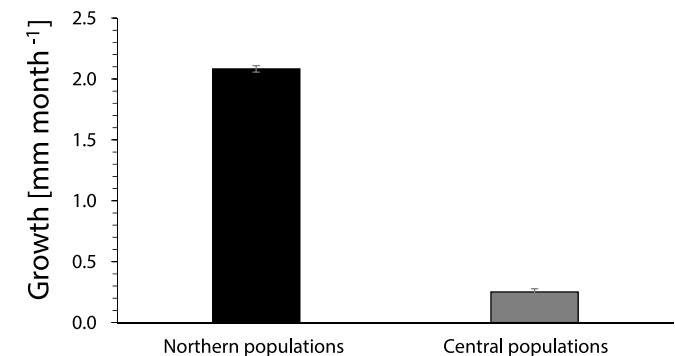


Fig. 4. Monthly linear growth rates [mm $month^{-1}$] (mean \pm SE) for northern ($n = 289$) and central ($n = 118$) populations of *Corallina officinalis* across its natural distribution in the NE Atlantic in summer conditions. Sample sizes vary in relation to staining success.

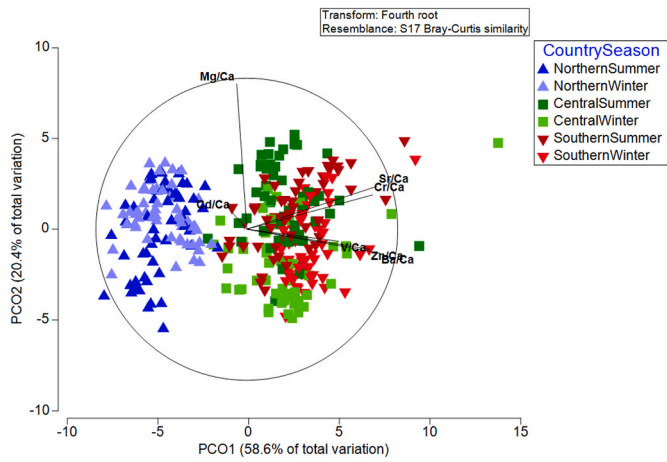


Fig. 5. PERMANOVA (2D stress: 0.17) with SIMPER results for all populations across the geographic distribution of *Corallina officinalis* across the NE Atlantic. Blue upward-facing triangles, green squares and red downward-facing triangles represent northern, central and southern populations, respectively. Seasonal differences are indicated in darker respective colours for summer and lighter respective colours for winter.

SP but rates of CP vs. SP are comparable (Kruskal-Wallis H test, $P = 0.025$ and $P = 0.035$, respectively; comparison within thallus regions). Mg/Ca ratios were directly compared with the physiological parameters of net production, respiration, net calcification and dark calcification (Fig. 7) and environmental parameters (Fig. S3; Kolzenburg et al., 2023).

V/Ca between seasons were not significantly different in any of the geographical regions. NP showed significantly lower V/Ca ratios between lower vs. middle and upper thallus regions (Kruskal-Wallis H test, $P = <0.036$ for all). Ratios of all but upper thallus regions of SP are significantly elevated compared to CP and NP (Kruskal-Wallis H test, $P = <0.022$ for all CP and $P = <0.001$ for all NP).

Cr/Ca of only CP showed a significant decrease from summer to winter in middle thallus regions and a significant positive increase in upper and lower thallus regions (Kruskal-Wallis H test, $P = <0.001$, for all). All thallus regions showed a highly significant increase in values from the NP to CP and SP (Kruskal-Wallis H test, $P = <0.001$ for all). When comparing SP and CP, the bottom and middle thallus regions showed a highly significant increase in values during winter (Kruskal-Wallis H test, $P = <0.001$ for both).

Fe/Ca showed high variability in all populations, seasons and thallus regions. Winter ratios showed a trend towards lower values in both leading and trailing edge populations as compared to central populations. No significant difference in any region or season was found between CP and SP, or between seasons for each region within a population. NP and CP showed significantly higher ratios at the tip as

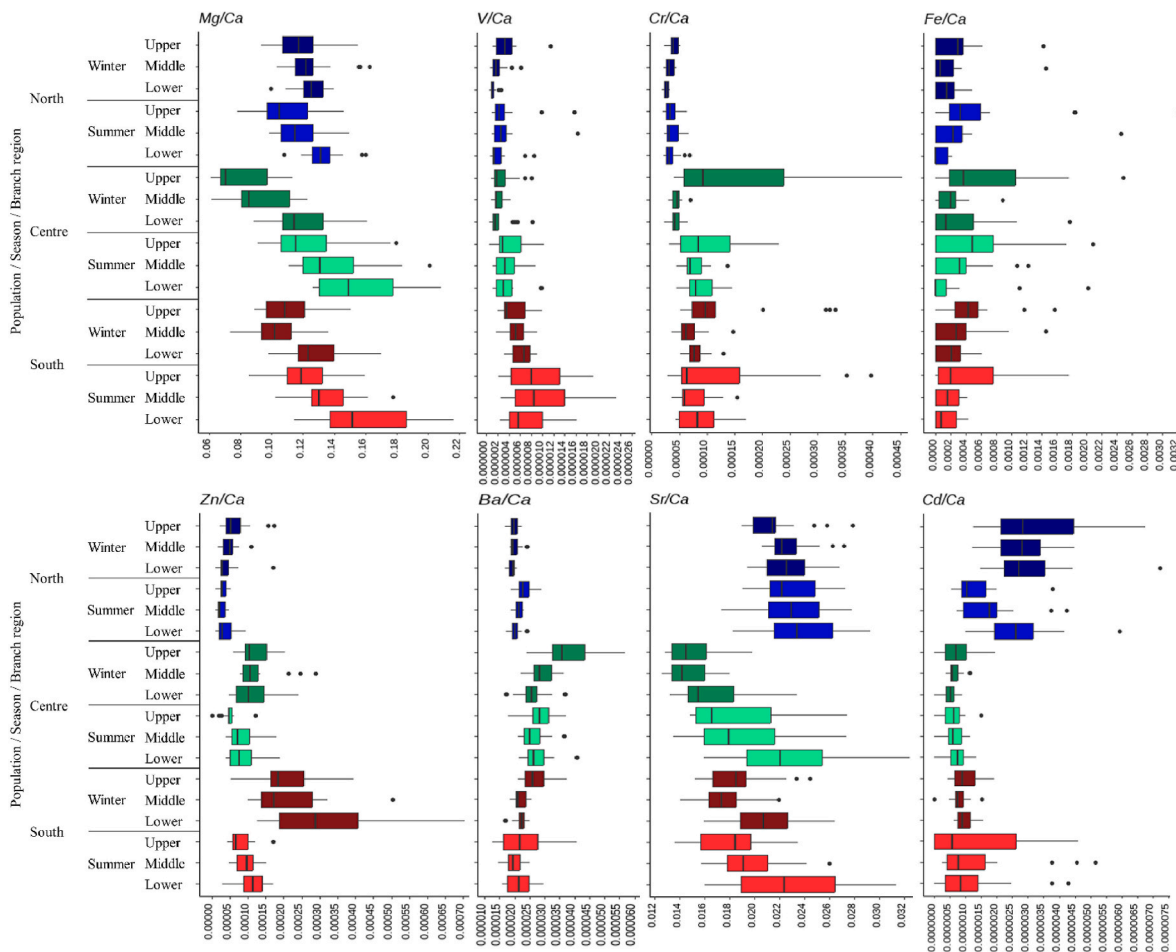


Fig. 6. Boxplots of element/Ca ratios for magnesium (Mg), vanadium (V), chromium (Cr), iron (Fe), zinc (Zn), barium (Ba), strontium (Sr) and cadmium (Cd) in different parts of the branch. The upper, middle and lower branch regions ($n = 9$) are nested within seasons (Winter, Summer) and seasons are nested within geographical regions (North, Centre and South). Northern, central and southern geographical regions are represented in blue, green and red, respectively. Seasons within the geographical region are differentiated by darker (winter) and lighter (summer) shades of the respective colour. All element ratios are based on ppm values.

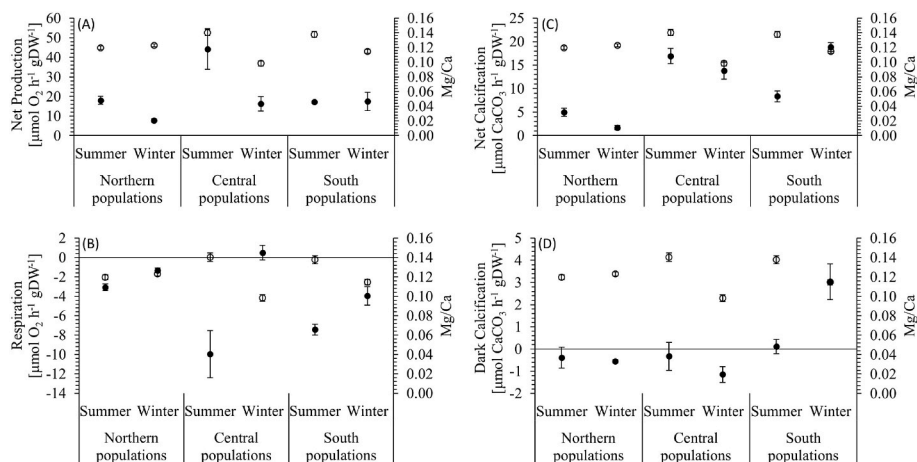


Fig. 7. (A) Net primary production [$\mu\text{mol O}_2 \text{ h}^{-1} \text{ gDW}^{-1}$] (mean \pm SE; closed circles), (B) respiration [$\mu\text{mol O}_2 \text{ h}^{-1} \text{ gDW}^{-1}$] (mean \pm SE; closed circles), (C) net calcification in the light [$\mu\text{mol CaCO}_3 \text{ h}^{-1} \text{ gDW}^{-1}$] (mean \pm SE; closed circles) and (D) calcification in the dark [$\mu\text{mol CaCO}_3 \text{ h}^{-1} \text{ gDW}^{-1}$] (mean \pm SE; closed circles) of *Corallina officinalis*. The secondary vertical axis shows Mg/Ca ratios (mean \pm SE; open circles in all graphs; element ratios are based on ppm values) of both populations from northern, central and southern locations along the latitudinal gradient in the NE Atlantic in summer and winter. Physiological parameters were previously published (Kolzenburg et al., 2023).

compared to the bottom of the thallus in both seasons (Kruskal-Wallis H test, $P = <0.048$ for all), except NP in winter.

Zn/Ca increased from North to South, following the same trend as Cr/Ca. Significant increases include NP vs. CP and vs. SP within a season in all thallus regions (Kruskal-Wallis H test, $P = <0.004$ for all, except the tip of CP in summer). Only SP showed significantly higher ratios within the lower thallus regions in winter as compared to summer

(Kruskal-Wallis H test, $P = 0.001$).

Sr/Ca decreased significantly from NP in higher latitudes to CP and SP in lower latitudes (Kruskal-Wallis H test, $P = <0.025$ for all, except for lower thallus regions). The same significant difference was found for CP vs. SP in winter (Kruskal-Wallis H test, $P = <0.040$ for all). All CP but neither the leading nor trailing edge population decreased significantly between seasons at each region of the thallus (Kruskal-Wallis H test, $P =$

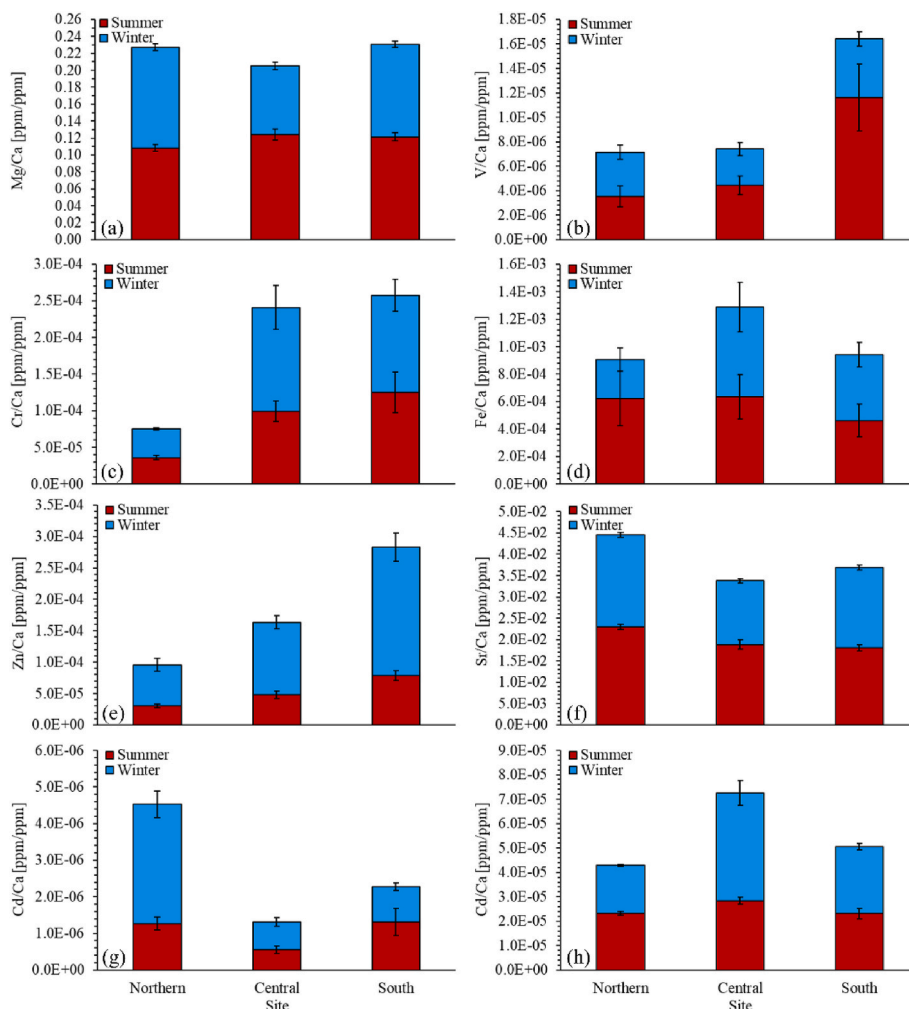


Fig. 8. Cumulative Element/Ca ratios [ppm/ppm] of the entire thallus of northern (leading edge), central and southern (trailing edge) populations in summer (red) and winter (blue) for (a) Mg/Ca, (b) V/Ca, (c) Cr/Ca, (d) Fe/Ca, (e) Zn/Ca, (f) Sr/Ca, (g) Cd/Ca and (h) Cd/Ca (mean \pm SE).

<0.009 for all). Sr/Ca ratios were also compared to their correlating environmental proxy, salinity (Fig. S3).

Cd/Ca significances between NP and other geographical locations were clearly differentiated, showing significantly higher ratios in NP as compared to CP and SP apart from the thallus tip of SP during summer (Kruskal-Wallis H test, $P = <0.028$ for all). No significant difference was found between CP and SP. Seasonal differences were only found in NP and expressed significantly or marginally significantly lower in summer as compared to winter (Kruskal-Wallis H test, $P = <0.001$ for the top region and $P = <0.057$ for the middle region).

Ba/Ca followed almost the opposite trend of Sr/Ca with significantly highest values in CP as compared to NP and SP across all thallus regions (Kruskal-Wallis H test, $P = <0.043$ for all), SP showed significantly higher values than NP in the upper and lower thallus regions in winter (Kruskal-Wallis H test, $P = <0.007$ for both). Significant differences between seasons were found within both leading and trailing edge populations in the upper thallus region during summer (Kruskal-Wallis H test, $P = <0.004$ for both). Ambient sampling details for correlations are summarised in Table S1. Ba/Ca ratios were also compared to their correlating environmental proxy, salinity (Fig. S3).

A cumulative representation of Element/Ca ratios for summer and winter of each geographical locality is represented in Fig. 8.

Main PERMANOVA analyses indicated that the chemical composition of *C. officinalis* cell walls was significantly different between countries (Co), location (Lo) (= region) on the thallus, 'seasons (Se) nested within country (Se(Co))' and 'season nested within country of location (Se(Co)xLo)' (PERMANOVA, $P < 0.001$ for all), indicating that the chemical composition of the ambient environment has a major effect on the cell wall elemental composition. Pairwise comparisons revealed significant seasonal differences within thallus region within a country (Se(Co)xLo for factor season in all but the bottom thallus of NP (PERMANOVA, $P < 0.017$ for all), between thallus locations within a country and between countries within thallus location (PERMANOVA, $P < 0.014$ for all; Table S8).

SIMPER analyses presented the main elemental composition and signature of each country's population. A clear separation between NP and SP was led by increased concentrations of Cd in NP but not CP or SP (Fig. 6, Table S9). Overall, 90.36%, 91.08% and 96.96% of the data were represented in SIMPER for NP, CP and SP, respectively. For NP, CP and SP 75.39%, 71.91% and 70.78%, respectively, of the data were concentrated in the most abundant elements Mg, Sr and Cr, in this order. The remaining major contributing elements were Zn and Ba. However, Zn and Ba contributions in this particular order were reversed in NP compared to CP and SP. While Cd dominated primarily in NP, Sr and Cr determined SP more so than CP.

4. Discussion

We investigated the structural and elemental traits of *C. officinalis* across its geographical distribution in the NE Atlantic. Due to the exposure to a wide range of abiotic and biotic factors, *C. officinalis* showed different local and seasonal adaptations to regions. Environmental parameters that are referred to in the discussion can be found in Table S1.

4.1. Trace element compositions

There is high compositional variability between all thallus regions. To interpret the data reliably, this discussion focuses mainly on the lower, more maturely calcified thallus region to eliminate potential differences in elemental incorporation at the younger and commonly less calcified apex of the specimen and account for real variability. Additionally, we are assuming that the signature reflects the usage and uptake of elements through physiological processes at the time of development. When comparing SIMPER findings with geological data, elevated concentrations of Cr and Mg, as found in trailing edge

populations, may be attributed to local substrate compositions which in NW Spain typically consist of Mg and Cr-rich ophiolites (Martínez et al., 2007).

In the calcite lattice, Mg^{2+} ions substitute Ca^{2+} ions with increasing temperatures, establishing a positive correlation between Mg content and Mg/Ca ratios with temperature (Kolesar, 1978; Milliman et al., 1971; Oomori et al., 1987). Studies have shown exponential temperature dependency of Mg uptake into calcite of 1–3 mol% per 1 °C increase depending on species (Henrich et al., 1996; Kamenos et al., 2008; Rosenthal et al., 1997). As for calcification, upper thallus regions of northern populations showed lower Mg incorporation and increased with thallus age (Egilsdottir et al., 2013; Johansen, 2018) which is in line with the results of this study. The lack of clearly observable differences in Mg/Ca ratios in northern populations between seasons can thus be explained by the limited temperature difference of 1 °C in intertidal and seasonal variations (Kolzenburg et al., 2023), this means results are overshadowed by the standard error of Mg/Ca ratios. The overlap makes it challenging to predict *in situ* and short-term developments in Mg/Ca ratios (Fig. S3). Similarly, Mg concentrations are comparable in central and southern populations, due to similar temperatures in the summer and winter, and are marginally higher in northern populations (Fig. 8). We agree with previous literature findings that Mg content presents a suitable proxy for substantial temperature changes, e.g. seasonal variations, and reconstruction in coralline algae (Kamenos et al., 2008). This was very clear for seasonality but due to the nature of the intertidal environment, a more detailed reconstruction between geographical localities was unsuccessful.

When relating skeletal Mg concentrations and the environmental carbonate system, coralline algae are expected to be negatively affected in their growth and calcification rates (Egilsdottir et al., 2013) and an alteration of their skeletal elemental composition along with a negative effect on its structure and structural integrity is expected (Ragazzola et al., 2012, 2013, 2016; Ries, 2011). This is mainly due to changing carbonate chemistry such as pH or dissolved inorganic carbon (DIC) levels in their natural environment and predicted future changes due to the uptake of anthropogenic CO_2 into the ocean surface layer. In addition to and in combination with the effects of increasing temperatures described above, studies have shown that this may cause coralline algae to lose some of their functions as ecosystem engineers and habitat formers due to alterations of structural properties within their calcite skeleton (Ragazzola et al., 2012). Interpreting the cumulative Mg/Ca ratios of both seasons from our study, we expect central populations, which showed overall lowest cumulative Mg/Ca ratios, to be somewhat more severely impacted by increased pCO_2 than leading and trailing edge populations. This may be due to potentially higher skeletal fracturing rates and damage to the epithelium of the alga which would normally protect it from dissolution which are thought to be caused by a reduced seawater pH (Ragazzola et al., 2012). Despite the latter study focusing on a crustose coralline algae, we would expect a very similar outcome for articulated coralline algae due to their structural similarities.

Ba/Ca, Cr/Ca, Zn/Ca and V/Ca ratios were lowest in northern populations. The only ratios which showed higher or comparable values than in the other locations were Cd/Ca, Sr/Ca and Mg/Ca. Ba/Ca, Cr/Ca and Fe/Ca are highest in central locations. Southern populations showed the highest values in Zn/Ca and V/Ca ratios.

Ba/Ca does reflect the environmental salinity levels measured at the locations to some extent, where southern locations show the highest salinities and were therefore expected to have the lowest Ba/Ca ratios (Lea et al., 1989). Ba/Ca ratios did not show the lowest but close to the lowest values in southern populations, jointly with northern populations which in turn might be exposed to heightened freshwater input from snow melt. In addition to this and due to the thermodynamically controlled uptake of Ba in the calcite lattice, as confirmed by lowest values in poleward populations, Ba/Ca ratios did prove valuable as an environmental proxy for freshwater input in articulated calcifying algae

and are suggested to also be useful for long-term monitoring as well as ambient measurements or historical reconstruction.

Values of Sr/Ca ratios mirror the decrease of salinity with increasing latitude due to increasing freshwater input along this gradient. Sr/Ca also closely follows Mg/Ca, implying, additionally following temperature trends.

Increased Cr levels can cause DNA and gene transcription modifications as well as growth and primary production inhibition (Sari and Tuzen, 2008). Concentrations of Cr are lower in all populations in winter than in summer, resulting in enhanced photosynthetic and growth inhibition in summer and in central and southern populations. This is also represented by greater growth rates in northern compared to central populations.

Central and southern populations' physiology is most heavily influenced by both the positive and negative effects of high Zn concentrations (Amado Filho et al., 1997; Longerich et al., 1996; Rout and Das, 2009), which is subsequently also reflected in reduced cell wall thickness. A general increase of skeletal Zn concentrations from summer to winter demonstrates the adaptations of organisms to increase net primary production (P_N) and therefore CO_2 assimilation under winter conditions. With temperature and light inhibition in the summer, southern populations may adapt by increasing the P_N rates in winter (Kolzenburg et al., 2023) through the utilization of the macronutrient.

Cd/Ca ratios of both leading and trailing edge locations, but especially in northern populations, indicate higher pollution rates and lower productivity, the inhibition of nutrient uptake and the prevention of calcite precipitation and photosynthetic activities (Kangwe et al., 2001; Vymazal, 1987). This was not only shown for algae in this study but also for terrestrial plants (Nazar et al., 2012) urging the potential detrimental effect on the majority of organisms. The effect of Cd coincides with P_N , gross primary production (P_G), respiration (R) and calcification data when comparing central, leading and trailing edge populations (Kolzenburg et al., 2023) Thick cell walls and fast growth in northern populations might contradict this finding, however, it might be due to adaptation to prolonged exposure to storms and thereby to potential mechanical damage, causing the organisms to prioritise cell wall thickness and sturdiness over primary production.

The limiting step during Fe incorporation is thermodynamically controlled (Johansen, 2018; Milliman et al., 1971; Raven et al., 1999), hence, a higher Fe/Ca rate is expected in southern populations. However, the highest rates were found in central followed by northern populations which are comparable to southern populations, presenting a high difference between central and northern/southern locations. A possible consequence of relatively low Fe in southern populations in combination with an increased concentration of Cd, which is known to inhibit nutrient uptake, may be physiological impairment.

V/Ca ratios highly likely demonstrate that northern populations are locally adapted to low light temperature conditions and do not need to build up and store chlorophyll *a* contents (Krenn et al., 1989; Meisch and Bauer, 1978; Meisch and Benzschawel, 1978; Wilhelm and Wild, 1984a, 1984b), contrary to southern populations.

Other studies (Yildiz et al., 2013) suggest that changes in the organisms' skeletal content might affect the ability of *C. officinalis* to absorb light, and increased exposure to ultraviolet radiation may change growth and photosynthetic performance. This hypothesis was supported by findings in our study and in combination with other studies (Kolzenburg et al., 2023).

A potential future skeletal softening due to changes in skeletal elemental compositions, most noticeably due to an increase in Mg/Ca ratios, in turn caused by thermal changes, may lead to a reduced resilience of *C. officinalis* to predicted future environmental conditions that are expected to be warmer, stormier and enhanced in terms of mechanical forces in the intertidal. These consequences of climate change may be exacerbated by the anthropogenic addition of toxic elements onto coastal environments through run-off and discharge, stressing *C. officinalis* and potentially other calcifying and non-calcifying

macroalgae and therefore potentially reducing their adaptation potential and resilience as well as associated biodiversity.

4.2. Structural integrity

Mg/Ca ratios and temperature are generally thought to be positively correlated with hardness, elasticity and crack resistance (Bianco-Stein et al., 2021; Kunitake et al., 2012; Long et al., 2014). Therefore, newly formed thallus sections are more elastic in winter due to lower Mg/Ca ratios and temperatures (Bianco-Stein et al., 2021; Long et al., 2014) and therefore most probably form a more elastic thallus over time as compared to thalli from central and trailing edge populations. Geniculated coralline algae have evolved to adapt to harsh intertidal environments with high tensile strength resistance and elasticity as a result of their segmented and jointed structure. This structure determines their location and survival on the rocky shores (Martone and Denny, 2008a) and can withstand high forces. Physical and ecological stress may cause damage to the organisms via cuts, scars or even holes in the frond. As already pointed out in other studies (Melbourne et al., 2015), little research was conducted on changes in the structural integrity of coralline algae, and it was mainly carried out on non-geniculate species apart from *Ellisolandia elongata* and very recently, *Corallina vancouveriensis* and *Calliarthron tuberculosum* (Guenther et al., 2022; Marchini et al., 2019).

We have shown that northern populations build thicker cell walls than southern and central populations, which are comparable to each other. Therefore, northern populations of the NE Atlantic need lower Mg concentrations within their skeleton to become more elastic and withstand abrasion due to autumn and winter storms (Kunitake et al., 2012; Long et al., 2014). This coincides with temperature and Mg/Ca measurements, which are the lowest in NP. The cell wall thickness also explains the greatest staining success for growth rate determination in northern as compared to central populations. Additional reasons for reduced staining success in central populations may be the lack of uptake or loss due to abrasion which was described for *C. officinalis* (Andrake and Johansen, 1980).

Intra-cell walls (perpendicular to growth direction) are thicker in all populations, indicating their important function for structural stabilization as well as protection of the cell interior. Due to their shorter and thicker design compared to inter-cell walls (parallel in relation to direction of growth), intra-cell walls can absorb, buffer and channel exogenous mechanical impacts through spreading. We speculate that thinner cell walls in central and southern populations compared to northern populations may be explained by shorter exposure to autumn, winter and potentially spring storms, thereby less exposure to potential mechanical damage. This also explains the greater difference between inter- and intra-cell wall thickness in southern, followed by central, followed by northern populations, and therefore firmer thalli in northern populations. The average cell wall thickness of all populations determined in this study independent from orientation lies within the reported literature values of $1.8 \pm 0.71 \mu\text{m}$ (Walsh et al., 2008).

Even though calcification rates in central populations are higher, cell walls are thinner which may be due to simultaneously increasing dissolution rates. As a result, G_N is increased (Kolzenburg et al., 2023) to compensate for dissolution. The lowest calcification rates in northern populations contrast with the fact that these populations build the thickest cell walls. Therefore, low P_N may be a result of focusing energy expenditure on cell wall formation.

Under conditions with exceeding optimal temperatures, biochemical components are becoming less efficient or even damaged (Eggert, 2012; Kordas et al., 2011), resulting in an expected decline in growth rates and calcification. Therefore, growth rates of southern populations would be expected to be similar to or lower than those of northern populations due to summer inhibition as well as an increased concentration of the growth-inhibiting element Cd in both leading and trailing edge populations. All these parameters, most probably in combination, may lead

to a reduction of coralline algae cover in tropical and subtropical ecosystems (Doney et al., 2009).

Very few studies have determined the biomechanics, such as tensile strength, stress and elasticity of articulated coralline algae in correlation with environmental parameters they are exposed to and can withstand, and none looked at leading or trailing edge populations (Denny and King, 2016a, 2016b; Guenther et al., 2022; Marchini et al., 2019; Martone, 2007; Martone and Denny, 2008a, 2008b; Melbourne et al., 2015; Ragazzola et al., 2012). This knowledge gap complicates the establishment of detailed predictions for the future of intertidal articulated coralline algae species.

In combination with the precipitation of the thickest cell walls, the ability of northern populations to withstand harsh physical winter conditions may also be exemplified in the slight positive trend showing the highest, however not significantly greater values for forces (F_{tu}) it can withstand before rupturing compared to other tested populations. Northern populations develop a greater surface area per geniculum ($7.25 \cdot 10^{-4} \pm 7.53 \cdot 10^{-5}$) as compared to central populations ($2.59 \cdot 10^{-4} \pm 2.09 \cdot 10^{-5}$), resulting in less localised stress and greater stress resistance in northern ($20.50 \pm 2.02 \text{ N mm}^{-2}$) as compared to central populations ($46.53 \pm 7.75 \text{ N mm}^{-2}$). With only slightly higher tensile strength characteristics in northern as compared to central populations between seasons, sites and the size of genicula it can be assumed that the size of genicula, is not of primary importance in this aspect of *C. officinalis* structural integrity. The combination of these aspects may be evidence of a positive correlation between genicula strength and cell wall thickness, based on overall stronger thalli, and that both, but only in combination and not the genicula by itself, makes up an essential part of the stability and resilience of this algae. It also suggests local adaptation to harsh environmental conditions in subarctic environments. The relation between genicula strength and cell wall thickness has only sporadically been investigated and found comparative stress values for *C. officinalis* of $31.7 \pm 2.0 \text{ MPa}$ ($= \text{N mm}^{-2}$) from similar environments in Vancouver Island in the Northeast Pacific (Janot and Martone, 2016; Martone, 2007). Limited studies on clusters of fronds in dry samples of *E. elongata* or other taxonomically related species to *C. officinalis* have shown values of stress around $\sigma_{max} = 5.4 \pm 0.5 \text{ MPa}$, with the maximum load or stress (σ_{max}) that can affect the joints defined as the maximum force per unit area before tissue rupture (Denny, 1988). This value and indications for other articulated coralline species mentioned above are a minimum of four times less than what we measured for wet *C. officinalis* specimens, indicating that dry testing is not representative of *in situ* genicula strength.

To keep frond stability, genicula are initiated at regular intervals by the medullary meristem and unlike intergenicula medullary cells, they elongate with age (Johansen, 2018). F_{tu} and ϵ were only measured as a combined value between genicula and intergenicula. All thalli tested, ruptured in the genicula, the joints which allow for flexible and rapid adjustments of thallus shapes and are primarily responsible for bending in moving waters (Aguirre et al., 2010). Previous studies on coralline species investigating F_{tu} resistance focussed on the rupture of genicula in a single thallus as experienced in this study and found a mean force to break the tenth genicula to be around 22.7 N in *Calliarthron cheilosporioides* (Martone and Denny, 2008a, 2008b). A study investigating the strength of thalli bundles found that *Ellisolandia elongata* in the Mediterranean can withstand maximum stress of 2.1 ± 0.4 up to $5.4 \pm 0.5 \text{ N mm}^{-2}$ (mean \pm SEM; $1 \text{ MPa} = 1 \text{ N mm}^{-2}$; Ragazzola et al., 2017). Values found in previous studies (Martone and Denny, 2008a, 2008b) are considerably higher than in our study, potentially due to the location of the specimens or differences in species characteristics, such as thickness. However, values for *E. elongata* are relatively similar which could be due to the closer taxonomic relationship between the species used in the latter and this study. A recent publication on two articulated coralline algae species revealed that the biomechanics of the genicula of neither species were greatly influenced by increased temperature and decreased pH levels (Guenther et al., 2022). This finding confirms our observation

that, independently of the tested populations and seasons, no differences in the capability to withstand strain, force and displacement were found.

The physiological (Kolzenburg et al., 2023) and structural properties of northern populations are distinctly different from central and southern populations; however, central populations are not always different to southern populations. Southern populations showed a lack of local physiological and structural adaptation culminating in survival rather than thriving within their current environment. This was also visually confirmed over a 4-year period working at the same sites when thriving healthy-looking Coralline turfs gradually bleached and disappeared, and only some purple patches within a blanketed white bleached area remained, which made any further sampling or incubations impossible (Kolzenburg, pers. observ.). This implies that southern populations are located at the margin of this species' favourable conditions. In the future, this could lead to a permanent decline and disappearance of *C. officinalis* in the southern locations in the NE Atlantic, which may be accelerated by predicted future climatic changes. This is exposing a north-to-south latitudinal gradient regarding the structural integrity of *C. officinalis* in the NE Atlantic. A similar gradient was also found by Yesson et al. (2018) in the genetic data of specimens close to sampling locations used in this study. The severe effects on *C. officinalis* could also lead to changes within the respective ecosystem due to missing important functions these algae would no longer perform. Its characterisation across the NE Atlantic validated the adaptation of *C. officinalis* to predominantly low light and temperature conditions.

Adaptations to predicted climatic changes will need to include metabolic (Kolzenburg et al., 2021) and structural processes. Shedding light on the structure of *C. officinalis* across geographical latitudes will help to accurately determine how it will be able to withstand climatic changes and with it, an increase in intensity and frequency of physical force exposure caused by coastal storm events.

Author statement

Regina Kolzenburg: Conceptualization, Data curation, Formal analysis, Investigation, Methodology, Project administration, Software, Validation, Visualization, Writing - original draft, Writing - review & editing; **Hugo Moreira:** Data curation, Formal analysis, Investigation, Methodology, Software, Writing - original draft, Writing - review & editing; **Craig Storey:** Methodology, Resources, Supervision, Writing - review & editing; **Federica Ragazzola:** Conceptualization, Funding acquisition, Project administration, Supervision, Writing - review & editing.

Declaration of competing interest

The authors declare that they have no known competing financial interests or personal relationships that could have appeared to influence the work reported in this paper.

Data availability

Data will be made available on request.

Acknowledgements

The authors would like to thank all volunteers for their help with fieldwork and the technical staff for their fantastic support.

Appendix A. Supplementary data

Supplementary data to this article can be found online at <https://doi.org/10.1016/j.marenvres.2023.106086>.

References

- Adey, W.H., Macintyre, I.G., 1973. Crustose coralline algae: a Re-evaluation in the geological Sciences. *GSA Bulletin* 84, 883–904.
- Aguirre, J., Perfecti, F., Braga, J.C., 2010. Integrating phylogeny, molecular clocks, and the fossil record in the evolution of coralline algae (Corallinales and Sporolithales, Rhodophyta). *Paleobiology* 36, 519–533.
- Amado Filho, G.M., Karez, C.S., Andrade, L.R., Yoneshigue-Valentin, Y., Pfeiffer, W.C., 1997. Effects on growth and accumulation of zinc in six seaweed species. *Ecotoxicol. Environ. Saf.* 37, 223–228.
- Anderson, M.J., Gorley, R.N., Clark, K.L., 2009. PRIMER 6 & PERMANOVA+. 6.1. 13 & 1.0. PRIMER-E Ltd, Plymouth, UK.
- Andrake, W., Johansen, H.W., 1980. Alizarin red dye as a marker for measuring growth in *Corallina officinalis* L. (Corallinales, Rhodophyta). *J. Phycol.* 16, 620–622.
- Bianco-Stein, N., Polishchuk, I., Lang, A., Atiyya, G., Villanova, J., Zaslansky, P., Katsman, A., Pokroy, B., 2021. Structural and chemical variations in Mg-calcite skeletal segments of coralline red algae lead to improved crack resistance. *Acta Biomater.* 130, 362–373.
- Chan, P., Halfar, J., Williams, B., Hetzinger, S., Steneck, R., Zack, T., Jacob, D.E., 2011. Freshening of the Alaska Coastal Current recorded by coralline algal Ba/Ca ratios. *J. Geophys. Res. Biogeosci.* 116.
- Chave, K.E., 1954a. Aspects of the biogeochemistry of magnesium 1. Calcareous marine organisms. *J. Geol.* 62, 266–283.
- Chave, K.E., 1954b. Aspects of the biogeochemistry of magnesium 2. Calcareous sediments and rocks. *J. Geol.* 62, 587–599.
- Chave, K.E., Wheeler Jr., B.D., 1965. Mineralogical changes during growth in the red alga, *Clathromorphum compactum*. *Science* 147, 621, 1979.
- Coull, B.C., Wells, J.B.J., 1983. Refugees from fish predation: experiments with phytal meiofauna from the New Zealand rocky intertidal. *Ecology* 64, 1599–1609.
- Darenougue, N., De Deckker, P., Eggins, S., Fallon, S., Payri, C., 2018. A record of mining and industrial activities in New Caledonia based on trace elements in rhodolith-forming coralline red algae. *Chem. Geol.* 493, 24–36.
- Davenport, J., Butler, A., Cheshire, A., 1999. Epifaunal composition and fractal dimensions of marine plants in relation to emersion. *J. Mar. Biol. Assoc. U. K.* 79, 351–355.
- Dayton, P., 1972. Toward an understanding of community resilience and the potential effects of enrichments to the benthos at McMurdo Sound, Antarctica. *Proc. Colloquium Conser. problems in Antarctica* 81–96.
- Denny, M., 1995. Predicting physical disturbance: mechanistic approaches to the study of survivorship on wave-swept shores. *Ecol. Monogr.* 65, 371–418.
- Denny, M., 1988. *Biology and the Mechanics of the Wave-Swept Environment*. Princeton University Press.
- Denny, M., Wethey, D., 2001. Physical processes that generate patterns in marine communities. In: Bertness, M.D., Gaines, S.D., Hay, M.E. (Eds.), *Marine Community Ecology*, pp. 3–37.
- Denny, M.W., King, F.A., 2016a. The extraordinary joint material of an articulated coralline alga. II. Modeling the structural basis of its mechanical properties. *J. Exp. Biol.* 219, 1843–1850.
- Denny, M.W., King, F.A., 2016b. The extraordinary joint material of an articulated coralline alga. I. Mechanical characterization of a key adaptation. *J. Exp. Biol.* 219, 1833–1842.
- Doney, S.C., Fabry, V.J., Feely, R.A., Kleypas, J.A., 2009. Ocean acidification: the other CO₂ problem. *Ann. Rev. Mar. Sci.* 1, 169–192.
- Eggert, A., 2012. Seaweed responses to temperature. *Seaweed biology: novel insights into ecophysiology. ecology and utilization* 47–66.
- Egilsdottir, H., Noisette, F., Noël, L.M.-L.J., Olafsson, J., Martin, S., 2013. Effects of p CO₂ on physiology and skeletal mineralogy in a tidal pool coralline alga *Corallina elongata*. *Mar. Biol.* 160, 2103–2112.
- Grahame, J., Hanna, F.S., 1989. Factors affecting the distribution of the epiphytic fauna of *Corallina officinalis* (L.) on an exposed rocky shore. *Ophelia* 30, 113–129.
- Guenther, R., Porcher, E.M.A., Carrington, E., Martone, P.T., 2022. Effects of temperature and pH on the growth, calcification, and biomechanics of two species of articulated coralline algae. *Mar. Ecol. Prog. Ser.* 700, 79–93.
- Halfar, J., Zack, T., Kronz, A., Zachos, J.C., 2000. Growth and high-resolution paleoenvironmental signals of rhodoliths (coralline red algae): a new biogenic archive. *J. Geophys. Res. Oceans* 105, 22107–22116.
- Henrich, L., Holz, R., Knepp, G., 1996. Physically based cooling line model to meet growing demands in temperature and flexibility. *Ironmak. Steelmak.* 23, 79–81.
- Hofmann, G.E., Evans, T.G., Kelly, M.W., Padilla-Gamiño, J.L., Blanchette, C.A., Washburn, L., Chan, F., McManus, M.A., Menge, B.A., Gaylord, B., 2014. Exploring local adaptation and the ocean acidification seascape—studies in the California Current Large Marine Ecosystem. *Biogeosciences* 11, 1053–1064.
- IBM Corp., 2021. SPSS Statistics for Windows.
- IPCC, 2023. Summary for policymakers. In: *Climate Change 2023: Synthesis Report. A Report of the Intergovernmental Panel on Climate Change. Contribution of Working Groups I, II and III to the Sixth Assessment Report of the Intergovernmental Panel on Climate Change*.
- Janot, K., Martone, P.T., 2016. Convergence of joint mechanics in independently evolving, articulated coralline algae. *J. Exp. Biol.* 219, 383–391.
- Jochum, K.P., Nohl, U., Herwig, K., Lammel, E., Stoll, B., Hofmann, A.W., 2005. GeoReM: a new geochemical database for reference materials and isotopic standards. *Geostand. Geoanal. Res.* 29, 333–338.
- Johansen, H.W., 2018. *Coralline Algae: a First Synthesis*. CRC press.
- Kamenos, N.A., Cusack, M., Moore, P.G., 2008. Coralline algae are global palaeothermometers with bi-weekly resolution. *Geochim. Cosmochim. Acta* 72, 771–779.
- Kangwe, J.W., Hellblom, F., Semesi, A.K., Mtolera, M.S.P., Bjork, M., 2001. Heavy metal inhibition of calcification and photosynthetic rates of the geniculate calcareous algae *Amphiroa tribulus*. *WIOMSA Book Series* 147–157.
- Kelaiser, B.P., Chapman, M.G., Underwood, A.J., 2001. Spatial patterns of diverse macrofaunal assemblages in coralline turf and their associations with environmental variables. *J. Mar. Biol. Assoc. U. K.* 81, 917–930.
- Kolesar, P.T., 1978. Magnesium in calcite from a coralline alga. *J. Sediment. Res.* 48, 815–819.
- Kolzenburg, R., Coaten, D.J., Ragazzola, F., 2023. Physiological characterisation of the calcified alga *Corallina officinalis* (Rhodophyta) from the leading to trailing edge in the Northeast Atlantic. *Eur. J. Phycol.* 58, 83–98.
- Kolzenburg, R., D'Amore, F., McCoy, S.J., Ragazzola, F., 2021. Marginal populations show physiological adaptations and resilience to future climatic changes across a North Atlantic distribution. *Environ. Exp. Bot.* 188, 104522.
- Kolzenburg, R., Nicastro, K.R., McCoy, S.J., Ford, A.T., Zardi, G.I., Ragazzola, F., 2019. Understanding the margin squeeze: differentiation in fitness-related traits between central and trailing edge populations of *Corallina officinalis*. *Ecol. Evol.* 9, 5787–5801.
- Kordas, R.L., Harley, C.D.G., O'Connor, M.I., 2011. Community ecology in a warming world: the influence of temperature on interspecific interactions in marine systems. *J. Exp. Mar. Biol. Ecol.* 400, 218–226.
- Krenn, B.E., Izumi, Y., Yamada, H., Wever, R., 1989. A comparison of different (vanadium) bromoperoxidases; the bromoperoxidase from *Corallina pilulifera* is also a vanadium enzyme. *Biochim. Biophys. Acta Protein Struct. Mol. Enzymol.* 998, 63–68.
- Kunitake, M.E., Baker, S.P., Estroff, L.A., 2012. The effect of magnesium substitution on the hardness of synthetic and biogenic calcite. *MRS Commun* 2, 113–116.
- Lea, D.W., Mashioita, T.A., Spero, H.J., 1999. Controls on magnesium and strontium uptake in planktonic foraminifera determined by live culturing. *Geochim. Cosmochim. Acta* 63, 2369–2379.
- Lea, D.W., Shen, G.T., Boyle, E.A., 1989. Coralline barium records temporal variability in equatorial Pacific upwelling. *Nature* 340, 373–376.
- Long, X., Ma, Y., Qi, L., 2014. Biogenic and synthetic high magnesium calcite—A review. *J. Struct. Biol.* 185, 1–14.
- Longerich, H.P., Jackson, S.E., Günther, D., 1996. Inter-laboratory note. Laser ablation inductively coupled plasma mass spectrometric transient signal data acquisition and analyte concentration calculation. *J. Anal. At. Spectrom.* 11, 899–904.
- Marchini, A., Ragazzola, F., Vasapollo, C., Castelli, A., Cerrati, G., Gazzola, F., Jiang, C., Langeneck, J., Manauzzi, M.C., Musco, L., 2019. Intertidal Mediterranean coralline algae habitat is expecting a shift toward a reduced growth and a simplified associated fauna under climate change. *Front. Mar. Sci.* 106.
- Martínez, S.S., Arenas, R., Andonaegui, P., Catalán, J.R.M., Pearce, J.A., 2007. Geochemistry of Two Associated Ophiolites from the Cabo Ortegal Complex (Variscan Belt of NW Spain).
- Martone, P.T., 2007. Kelp versus coralline: cellular basis for mechanical strength in the wave-swept seaweed *Calliarthron* (Corallinales, Rhodophyta). *J. Phycol.* 43, 882–891.
- Martone, P.T., Alyono, M., Stites, S., 2010. Bleaching of an intertidal coralline alga: untangling the effects of light, temperature, and desiccation. *Mar. Ecol. Prog. Ser.* 416, 57–67.
- Martone, P.T., Denny, M.W., 2008a. To bend a coralline: effect of joint morphology on flexibility and stress amplification in an articulated calcified seaweed. *J. Exp. Biol.* 211, 3421–3432.
- Martone, P.T., Denny, M.W., 2008b. To break a coralline: mechanical constraints on the size and survival of a wave-swept seaweed. *J. Exp. Biol.* 211, 3433–3441.
- Martone, P.T., Janot, K., Fujita, M., Wasteneys, G., Ruel, K., Joseleau, J.-P., Estevez, J.M., 2019. Cellulose-rich secondary walls in wave-swept red macroalgae fortify flexible tissues. *Planta* 1867–1879. <https://doi.org/10.1007/s00425-019-03269-1>.
- McCoy, S.J., Widdicombe, S., 2019. Thermal plasticity is independent of environmental history in an intertidal seaweed. *Ecol. Evol.* 9, 13402–13412.
- Meisch, H.-U., Bauer, J., 1978. The role of vanadium in green plants: IV. Influence on the formation of δ -aminolevulinic acid in *Chlorella*. *Arch. Microbiol.* 117, 49–52.
- Meisch, H.-U., Benzschawel, H., 1978. The role of vanadium in green plants: III. Influence on cell division of *Chlorella*. *Arch. Microbiol.* 116, 91–95.
- Melbourne, L.A., Griffin, J., Schmidt, D.N., Rayfield, E.J., 2015. Potential and limitations of finite element modelling in assessing structural integrity of coralline algae under future global change. *Biogeosciences* 12, 5871–5883.
- Milliman, J.D., Gastner, M., Müller, J., 1971. Utilization of magnesium in coralline algae. *Geol. Soc. Am. Bull.* 82, 573–580.
- Moberly Jr., R., 1968. Composition of magnesian calcites of algae and pelecypods by electron microprobe analysis 1. *Sedimentology* 11, 61–82.
- Nazar, R., Iqbal, N., Masood, A., Khan, M.I.R., Seyed, S., Khan, N.A., 2012. Cadmium Toxicity in Plants and Role of Mineral Nutrients in its Alleviation.
- Noël, L.M.-L.J., Hawkins, S.J., Jenkins, S.R., Thompson, R.C., 2009. Grazing dynamics in intertidal rockpools: connectivity of microhabitats. *J. Exp. Mar. Biol. Ecol.* 370, 9–17. <https://doi.org/10.1016/j.jembe.2008.11.005>.
- Oomori, T., Kaneshima, H., Maezato, Y., Kitano, Y., 1987. Distribution coefficient of Mg²⁺ + ions between calcite and solution at 10–50 °C. *Mar. Chem.* 20, 327–336.
- Paton, C., Hellstrom, J., Paul, B., Woodhead, J., Hergt, J., 2011. Iolite: freeware for the visualisation and processing of mass spectrometric data. *J. Anal. At. Spectrom.* 26, 2508–2518.
- Pereira, N.S., Voegelin, A.R., Paulukat, C., Sial, A.N., Ferreira, V.P., Frei, R., 2016. Chromium-isotope signatures in scleractinian corals from the Rocas A toll, Tropic S outh Atlantic. *Geobiology* 14, 54–67.

- Ragazzola, F., Foster, L.C., Form, A., Anderson, P.S.L., Hansteen, T.H., Fietzke, J., 2012. Ocean acidification weakens the structural integrity of coralline algae. *Global Change Biol.* 18, 2804–2812.
- Ragazzola, F., Foster, L.C., Form, A.U., Büscher, J., Hansteen, T.H., Fietzke, J., 2013. Phenotypic plasticity of coralline algae in a high CO₂ world. *Ecol. Evol.* 3, 3436–3446.
- Ragazzola, F., Foster, L.C., Jones, C.J., Scott, T.B., Fietzke, J., Kilburn, M.R., Schmidt, D. N., 2016. Impact of high CO₂ on the geochemistry of the coralline algae *Lithothamnion glaciale*. *Sci. Rep.* 6, 1–9.
- Ragazzola, F., Raiteri, G., Fabbri, P., Scafe, M., Florio, M., Nannini, M., Lombardi, C., 2017. Structural integrity of *Ellisolandia elongata* reefs: a mechanical approach to compare tensile strengths in natural and controlled environments. *Mar. Ecol.* 38, e12455.
- Rasband, W.S., 2016. ImageJ.
- Raven, J.A., Evans, M.C.W., Korb, R.E., 1999. The role of trace metals in photosynthetic electron transport in O₂-evolving organisms. *Photosynth. Res.* 60, 111–150.
- Ries, J.B., 2011. Skeletal mineralogy in a high-CO₂ world. *J. Exp. Mar. Biol. Ecol.* 403, 54–64.
- Rosenthal, Y., Boyle, E.A., Slowey, N., 1997. Temperature control on the incorporation of magnesium, strontium, fluorine, and cadmium into benthic foraminiferal shells from Little Bahama Bank: prospects for thermocline paleoceanography. *Geochem. Cosmochim. Acta* 61, 3633–3643.
- Rout, G.R., Das, P., 2009. Effect of metal toxicity on plant growth and metabolism: I. Zinc. *Sustain. Agri.* 873–884.
- Saha, N., Webb, G.E., Zhao, J.-X., 2016. Coral skeletal geochemistry as a monitor of inshore water quality. *Sci. Total Environ.* 566, 652–684.
- Sari, A., Tuzen, M., 2008. Biosorption of total chromium from aqueous solution by red algae (*Ceramium virgatum*): equilibrium, kinetic and thermodynamic studies. *J. Hazard Mater.* 160, 349–355.
- Schoene, B.R., Zhang, Z., Jacob, D., Gillikin, D.P., Tütken, T., Garbe-Schönberg, D., McConnaughey, T., Soldati, A., 2010. Effect of organic matrices on the determination of the trace element chemistry (Mg, Sr, Mg/Ca, Sr/Ca) of aragonitic bivalve shells (*Arctica islandica*)—comparison of ICP-OES and LA-ICP-MS data. *Geochem. J.* 44, 23–37.
- Steneck, R.S., 1986. The ecology of coralline algal crust: convergent patterns and adaptative strategies. *Annu. Rev. Ecol. Systemat.* 17, 273–303. <https://doi.org/10.1146/ANNUREV.ES.17.110186.001421>.
- Tavares, A.I., Nicastró, K.R., Kolzenburg, R., Ragazzola, F., Jacinto, R., Zardi, G.I., 2018. Isolation and characterization of nine microsatellite markers for the red alga *Corallina officinalis*. *Mol. Biol. Rep.* 45, 2791–2794.
- Tuzen, M., Verep, B., Ogretmen, A.O., Soylak, M., 2009. Trace element content in marine algae species from the Black sea, Turkey. *Environ. Monit. Assess.* 151, 363–368.
- Vinogradov, A., 1953. *The Elementary Composition of Marine Organisms*, vol. 2. Sears Foundation for Marine Research Mem.
- Vymazal, J., 1987. Toxicity and accumulation of cadmium with respect to algae and cyanobacteria: a review. *Toxic. Assess.* 2, 387–415.
- Walsh, P.J., Buchanan, F.J., Dring, M., Maggs, C., Bell, S., Walker, G.M., 2008. Low-pressure synthesis and characterisation of hydroxyapatite derived from mineralised red algae. *Chem. Eng. J.* 137, 173–179.
- Wilhelm, C., Wild, A., 1984a. The variability of the photosynthetic unit in *Chlorella I*. The effect of vanadium on photosynthesis, productivity, P-700 and cytochrome f in undiluted and homocontinuous cultures of *Chlorella*. *J. Plant Physiol.* 115, 115–124.
- Wilhelm, C., Wild, A., 1984b. The variability of the photosynthetic unit in *Chlorella II*. The effect of light intensity and cell development on photosynthesis, P-700 and cytochrome f in homocontinuous and synchronous cultures of *Chlorella*. *J. Plant Physiol.* 115, 125–135.
- Williamson, C.J., Brodie, J., Goss, B., Yallop, M., Lee, S., Perkins, R., 2014. *Corallina* and *Ellisolandia* (Corallinales, Rhodophyta) photophysiology over daylight tidal emersion: interactions with irradiance, temperature and carbonate chemistry. *Mar. Biol.* 161, 2051–2068.
- Yesson, C., Jackson, A., Russell, S., Williamson, C.J., Brodie, J., 2018. SNPs reveal geographical population structure of *Corallina officinalis* (Corallinaceae, Rhodophyta). *Eur. J. Phycol.* 53, 180–188.
- Yildiz, G., Hofmann, L.C., Bischof, K., Dere, Ş., 2013. Ultraviolet radiation modulates the physiological responses of the calcified rhodophyte *Corallina officinalis* to elevated CO₂. *Bot. Mar.* 56, 161–168.